19. The $V_\beta 1$ promoter fragment was generated by exonuclease III digestion. It extends from −1544 to +18 relative to the transcription start site as determined by S1 nuclease mapping. Activity of the $V_\beta 1$ promoter appears to be T cell–specific based on its stimulation of CAT activity when introduced upstream of the CAT gene in the vector CAT-RSVE.
20. F. Hochstenbach and M. B. Brenner, *Nature* **340**, 562 (1989).
21. J. M. Redondo and M. S. Krangel, unpublished results.
22. Activation by the RSVE fragment was also weak in these T cell lines. Thus, weak activation by the 1.4-kb Xba I fragment may reflect factors other than its intrinsic activity.
23. R. Sen and D. Baltimore, *Cell* **46**, 705 (1986).
24. A. Ephrussi, G. M. Church, S. Tonegawa, W. Gilbert, *Science* **227**, 134 (1985).
25. P. Sassone-Corsi and E. Borrelli, *Trends Genet.* **2**, 215 (1986).
26. Y. Shirayoshi, P. A. Burke, E. Appella, K. Ozato, *Proc. Natl. Acad. Sci. U.S.A.* **85**, 5888 (1988).
27. A. Winoto and D. Baltimore, *Cell* **59**, 649 (1989).
28. ———, *Nature* **338**, 430 (1989).
29. S. Takeshita, M. Toda, H. Yamagishi, *EMBO J.* **8**, 3261 (1989).
30. F. W. Alt, T. K. Blackwell, G. D. Yancopoulos, *Science* **238**, 1079 (1987).
31. M. Schlissel and D. Baltimore, *Cell* **58**, 1001 (1989).
32. C. M. Gorman, L. F. Moffat, B. H. Howard, *Mol. Cell. Biol.* **2**, 1044 (1982).
33. P. A. Luciw, J. M. Bishop, H. E. Varmus, M. R. Capecchi, *Cell* **33**, 705 (1983).
34. J. D. Dignam, R. M. Lebovitz, R. G. Roeder, *Nucleic Acids Res.* **11**, 1475 (1983).
35. W. Lee, P. Mitchell, R. Tjian, *Cell* **49**, 741 (1987).
36. We thank C. Doyle, S. Speck, E. Flemington, M. Woisetschlaeger, D. Diamond, A. Winoto, R. Guigo, and B. Alarcon for contributing reagents and for helpful discussions. Supported by a grant from NIH (R01-GM41052) and a Doctores y Tecnologos fellowship from the Ministerio de Educacion y Ciencia Español (to J.M.R.).

21 November 1989; accepted 6 February 1990

The Direction of Membrane Lipid Flow in Locomoting Polymorphonuclear Leukocytes

JULIET LEE, MIKAEL GUSTAFSSON, KARL-ERIC MAGNUSSON, KEN JACOBSON*

The objective of this study was to determine the direction of membrane lipid flow in locomoting cells. The plasma membrane of human polymorphonuclear leukocytes was stained with a fluorescent lipid analog dihexadecanoyl indocarbocyanine. A line was photobleached on the cell surface perpendicular to the direction of cell motion. Low–light-level fluorescence microscopy and digital image-processing techniques were used to analyze a series of images taken at short intervals after photobleaching. The bleached line remained visible for about 5 seconds before being erased by diffusional recovery. Examination of fluorescence intensity profiles allowed a comparison to be made between the velocities of line and cell movement. Results indicate that the bleached line moves forward with the same velocity as the cell during locomotion, refuting the retrograde lipid flow model of locomotion. Instead, the plasma membrane lipid appears to move forward according to either the unit movement of membrane or the tank track model of locomotion.

A KEY TO UNDERSTANDING THE MOlecular basis of cell locomotion lies in investigating the dynamics of membrane and cytoskeletal molecules during cell movement. Early approaches to this problem revealed the rearward movement of particles attached to the surface of moving cells (*1*). Patched or cross-linked membrane proteins were also found to display the same behavior in motile cells, the most familiar example being the phenomenon of capping (*2*). Recent advances in the field of digitized video microscopy permit the dynamics of well-characterized classes of proteins to be visualized in locomoting cells over extended periods of time (*3–5*), including the rearward movement of specific fluorescently labeled membrane proteins (*6, 7*). Submicron gold particles coated with either lectins, polylysine, or monoclonal antibodies have also been used to track the movements of membrane constituents (*8–10*).

Information about the movement of membrane components has been used to support several very different models of cell locomotion (*11–13*). These models differ on how the forces underlying membrane protein movement and cell locomotion are generated. The idea that the cytoskeleton is responsible for the rearward movement of membrane proteins (*13–15*) is supported by a considerable amount of experimental evidence (*2, 5, 7, 16, 17*). This cytoskeletal-driven process is regarded as part of the locomotory mechanism. Thus, it may be envisaged that when rearward-moving membrane proteins on the ventral cell surface become anchored to the substratum, continuation of a rearward-directed cytoskeletal force will tend to pull the cell forward.

An alternative explanation for the rearward movements of membrane proteins is the retrograde lipid flow (RLF) hypothesis (*12*). In this model, which has previously been used to explain the rearward movements of particles on the surface of moving cells (*1*), a rearward lipid flow exists on the dorsal and ventral cell surfaces that sweeps slowly diffusing membrane proteins or attached particles from the front to the rear of the cell. A rearward lipid flow is thought to be generated by the insertion of new membrane lipid (source) at the tip of the leading lamella, and the endocytosis of membrane lipid (sink) at sites randomly distributed over the cell surface. The cell is thought to advance by inserting new membrane lipid at the tip of the extending lamella. However, there has been no direct information about the direction of lipid flow in locomoting cells. All information regarding flow has been inferred from studies of particle movement on the surface of motile cells (*1, 9*). Therefore, an essential step toward building more realistic models of cell locomotion is to determine the direction of lipid flow directly in moving cells.

We have developed a method to detect the direction of plasma-membrane lipid flow during cell locomotion. We trace the movement of a mark created by photobleaching fluorescent lipid molecules embedded in the membrane of moving cells. A fluorescent lipid analog, dihexadecanoyl-indocarbocyanine (diI), was used to stain the membrane lipid of human polymorphonuclear leukocytes (PMNs). A pulse of laser light was then used to destroy the fluorescence within a discrete band across the cell, perpendicular to its direction of motion. Movement of the bleached line was recorded at short intervals after photobleaching (Fig. 1). However, this line is only temporary, since it is rapidly erased (within 5 s) by diffusion of unbleached fluorophores into the bleached region. Thus, the success of the experiment depends heavily on the degree of cell motility. Only in rapidly moving cells can line movement be detected before diffusional recovery is complete. Human PMNs are particularly suitable for this study as they can be highly motile on a glass substratum after staining with diI and are resilient to the effects of photobleaching in the presence of diI. A single cell may be photobleached up to five times without any apparent impairment of cell mobility or viability. One concern about this procedure is that membrane-bound diI is gradually internalized. Thus

J. Lee and K. Jacobson, Department of Cell Biology and Anatomy and Lineberger Cancer Research Center, University of North Carolina at Chapel Hill, Chapel Hill, NC 27599.
M. Gustafsson and K.-E. Magnusson, Department of Medical Microbiology, University of Linköping, Linköping, Sweden.

*To whom correspondence should be addressed.

line movement could be attributed to cytoplasmic flow and not solely to the movement of membrane lipid. However, confocal microscopy shows that there is no significant internalization of dil during the experimental time period (Fig. 2). This result confirmed previous observations of stained cells using a fluorescence microscope with a lens of high numerical aperture (1.4). By this means some degree of "optical sectioning" was obtained that made it possible to identify and exclude those cells from the experiment that had obviously internalized unacceptable amounts of dil.

The PMNs were bleached across the front edge during extension of the leading lamella or across the rear end during retraction of the trailing edge. Digitized, processed fluorescence images (Fig. 3, a to d) were used to create fluorescence intensity profiles (Fig. 3, e to h). These were used to calculate the velocity of the bleached line and the nearest cell margin, relative to the substratum (Fig. 1). The most striking observation was that a line bleached at either the front or rear of the cell moved with about the same velocity as the closest cell margin (Fig. 4, a and c). However, no line movement was observed in stationary cells.

The movement of PMNs is discontinuous, typically displaying episodes of rapid movement followed by periods of slower locomotion or no movement. Individual locomotion rates varied widely from 15 to 35 μm/min. To account for differences in cell locomotion speed, the normalized relative velocity of the bleached line (R) was calculated. This value was obtained by subtracting the bleached line velocity from that of the leading lamella (or retracting edge) and then dividing the difference by the velocity of the nearest moving cell margin (Fig. 4, b and d). When R is not equal to zero, a forward ($R < 0$) or rearward shift ($R > 0$) of the bleached line with respect to the nearest cell margin is indicated. However, our results gave a normalized relative velocity of approximately zero for both front and rear line bleaches. Thus these bleached lines moved in concert with their nearest cell margins in relation to the substratum but were stationary with respect to the cell surface (*18*).

In our considerations of bleached line movement so far, we refer to both dorsal and ventral cell surfaces because they will be bleached by about the same extent under the conditions of this experiment (*19*). Although both surfaces may be assumed to be

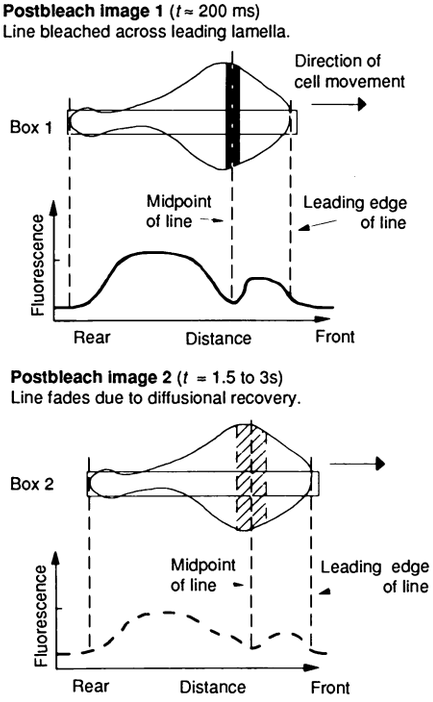

Fig. 1. Schematic representation of the photobleaching experiment. Low–light-level fluorescence images of moving cells (*25*) were acquired with a Nikon Diaphot inverted microscope (objective ×40) in conjunction with the same imaging system, data processing software, and procedures as described previously (*26, 27*). Line photobleaching was performed by passing 515-nm laser light through a cylindrical lens, focused on an intermediate image plane and then focused through the microscope objective, in order to produce a slitlike image on the cell surface of e^{-2} width = 4 μm. Duration of photobleaching was between 300 and 400 ms. As illustrated in this diagram, a line was photobleached across a leading lamella during extension. A series of four digitized fluorescence images consisting of a prebleach image and three postbleach images were usually collected to record the movement and recovery of the bleached line during cell locomotion; only the first two postbleach images are shown here. The same procedure was used for bleaching the rear of the cell during retraction. Postbleach images 1 and 2 were collected almost immediately after photobleaching and after 1.5 to 3.0 s, respectively. Fluorescence intensity profiles were created by averaging the fluorescence across each row of pixels perpendicular to the long axis of a rectangle defined parallel to the direction of cell movement. Inspection of fluorescence intensity profiles 1 and 2 gives the distance moved by the bleached line, the leading lamella, and the rear of the cell within a certain time interval. Thus, the velocities of these regions may be calculated with respect to a fixed point on the substratum. The time interval between postbleach images 1 and 2 depends on the speed of cell locomotion. This interval must be long enough to permit the detection of line movement, but before significant erasure of the line due to diffusional recovery.

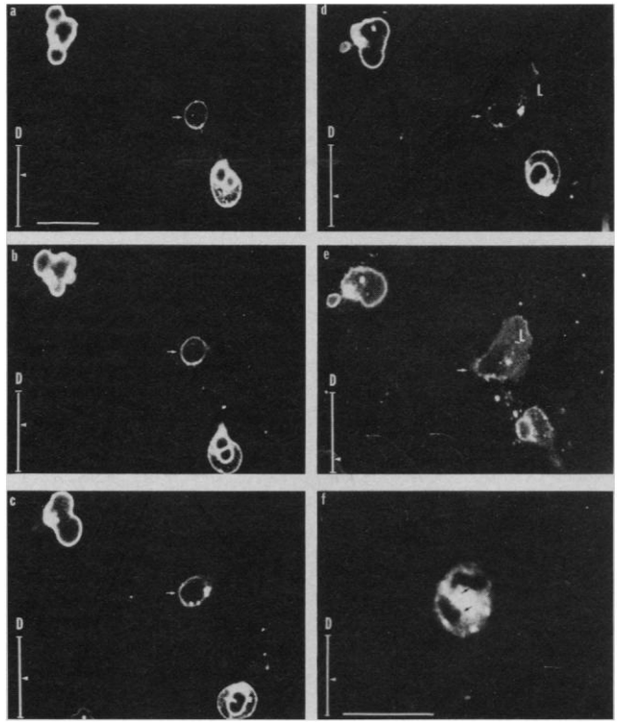

Fig. 2. Confocal microscopy of stained PMNs. (**a** to **e**) Part of a confocal series of images (*28*) obtained for PMNs incubated for 40 min after staining, starting at the dorsal surface (D) and continuing down at 0.5- to 1.0-μm intervals to the ventral surface. The step size and relative position of each section is indicated (arrow) by a vertical bar representing 8 μm (not to scale). The horizontal bar represents 20 μm. The distinctive "ring" staining of one cell (arrowed) is indicative of dil being present mainly on the cell surface. Note the changing contours of the ring as sections become more ventral indicating the complex morphology of these cells. The lamellar region (L) is extremely thin (~0.5 μm) as indicated by this region being visible only in the ventralmost sections. In panel (e), diffuse fluorescence can be seen over the entire lamella. Since this region is very thin, precise "optical sectioning" here is beyond the resolution of the confocal microscope. We attribute this diffuse staining to slightly out-of-focus fluorescence coming from both dorsal and ventral surfaces of the lamella and not to internalized dil. This staining pattern is also observed on the leading lamella of highly spread fibroblasts (*29*). (**f**) A confocal section (2 μm from dorsal surface) through a cell incubated for 1½ hours after staining. Vertical bar represents 3.5 μm; horizontal bar represents 20 μm. Here dil has clearly been internalized as shown by the bright fluorescence in the cytoplasmic region and the absence of ring staining. A particularly striking feature is the dark lobular structure (arrowed) inside the cell, which represents the multilobed nucleus and is a region from which dil is excluded. This feature is not seen in panels a to e. We conclude that there is no detectable internalization of dil within 40 min but significant internalization can occur after 1½ hours at 37°C. All experimental data was collected within 40 min after staining.

moving together, the real situation may be more complex, since one surface may be moving at a different velocity relative to the other. We tested this possibility, since this information would be of importance in the interpretation of our results with respect to the various models of cell locomotion. Because of the experimental difficulties of bleaching one surface only, computer simulation (*6*) was used to create fluorescence intensity profiles that would result from the recovery of bleached lines on two closely opposed surfaces moving at different relative velocities. A significant amount of line "broadening" (prior to the emergence of two separate lines) during diffusional recovery would suggest relative movement between dorsal and ventral cell membranes. However, our simulations revealed that significant broadening of the bleached line would not be detectable within the period of diffusional recovery for cells moving at less than 60 μm/min (*20*). Therefore, the possibility remains that some relative movement between dorsal and ventral membranes is occurring but is not detected with the present experimental procedure.

These results directly demonstrate lipid flow in moving cells and allow partial discrimination between three possible models of cell locomotion. Our interpretation of the results is centered on the movement of the midpoint of a bleached line across the leading lamella, since this is most pertinent to cell advancement. The predicted movement of a bleached line with respect to the leading lamella, according to each model of cell locomotion, is illustrated in Fig. 5.

According to the RLF model, the membrane lipid on both dorsal and ventral surfaces flows rearward. Thus, a line bleached across the leading lamella would be expected to move rearward with respect to the leading edge, having a normalized relative velocity equal to or greater than three (*21*). Another possibility is illustrated by the tank track model [(*11*), Fig. 5]. Here the membrane lipid on the dorsal surface moves forward at twice the speed of the cell while the ventral surface remains stationary as the cell advances. A line bleached on the dorsal surface only would be expected to move forward in relation to the leading lamella with a normalized relative velocity, R of -1 (*22*). In the unit movement of membrane model, we propose that both dorsal and ventral cell surfaces move forward as a unit during extension of the leading lamella. Similarly, when the rear of the cell retracts, both cell surfaces move forward together. This model suggests that the membrane lipid undergoes bulk movement that is tightly coupled to cell locomotion but without any forward or rearward shifts with respect to the cell surface. A line bleached on the surface of such a cell would be expected to show no movement with respect to the leading lamella and to have a normalized relative velocity of zero.

Thus it appears that our results agree best with the unit movement of membrane model since the normalized relative velocity of front (and rear) line bleaches is about zero. However, although our data are inconsistent with the retrograde lipid flow model, we cannot completely exclude the tank track

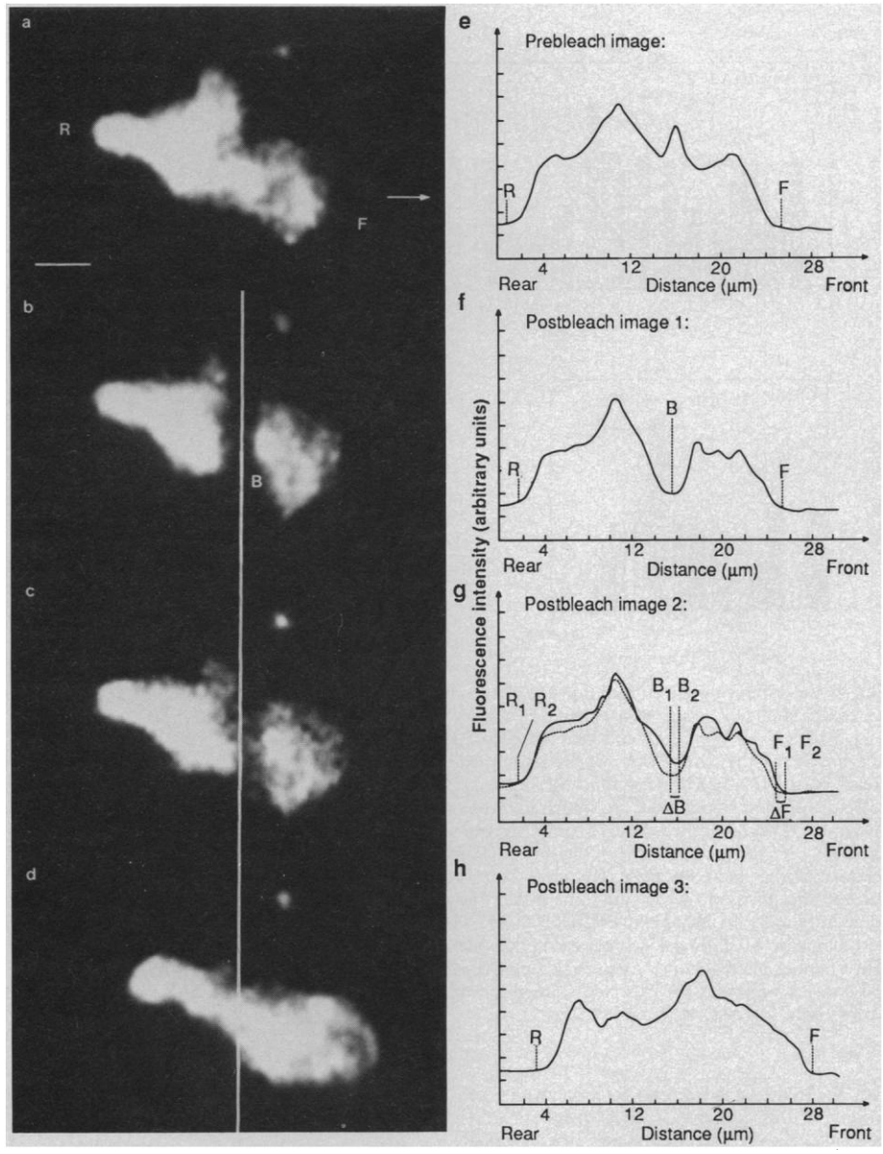

Fig. 3. "Front" bleach of PMN during extension of the leading lamella. (**a** to **d**) A complete set of digitized, fluorescence images, each the average of four successive frames. (a) The prebleach image; (b) postbleach image 1 acquired almost immediately after photobleaching; (c) postbleach image 2 acquired 1.7 s after photobleaching; (d) final image showing complete fluorescence recovery and the final position of the cell. The direction of motion is marked (arrow) as is the front of the cell (F), rear (R), and the bleached line (B). A vertical line bisects the original position of the midpoint of the bleached line. It passes through the same coordinates with respect to the substratum in each image. Note the forward shift of the bleached line relative to the vertical line, (b and c), together with the forward movement of the front edge of the cell. Bar = 5 μm; 1 pixel = 0.207 μm. (**e** to **h**) The fluorescence intensity profiles corresponding to images a to d. The front of the cell (F), rear (R), and midpoint of the bleached line (B) are marked as before. A comparison of e and f shows that the bleached line leads to a marked trough in the fluorescence intensity profile that cannot be mistaken for a normally occurring fluctuation in the surface fluorescence of an unbleached cell. The profile of the bleached line becomes shallower as diffusional recovery occurs (compare f and g). Panel g shows the profile of postbleach image 1 (dotted line) superimposed on postbleach image 2. From this example it can be seen that the distance moved by the front of the cell (delta F) is the same as the distance moved by the bleached line (delta B). However, the rear of the cell remains stationary (delta $R = 0$) but had clearly moved forward by the time postbleach image 3 was acquired.

model because we are unable to detect relative movement between the dorsal and ventral cell membranes, in terms of bleached line broadening during the time course of this experiment. Furthermore, according to the tank track model, a bleached line will initially consist of a superimposition of a dorsal surface bleach moving at twice the cell velocity and a stationary ventral surface bleach. Computer simulation shows that for short times after photobleaching, this composite bleached line becomes broader and its midpoint appears to move with the same velocity as the cell and so would be indistinguishable from the movement of the midpoint of a bleached line according to the unit movement of membrane model. Nevertheless, evidence in favor of the unit movement of membrane model comes from gold particle tracking of lectin and extracellular matrix receptors on the surface of rapidly moving keratocytes (*23*). A certain class of receptors was found to move forward with the same velocity as the cell but show no net movement with respect to the cell surface. This result would appear to suggest that the membrane lipid bilayer does indeed move forward in concert with the cell during locomotion. However, a demonstration that some of these receptors are associated with membrane lipid molecules is required before a full distinction between the unit movement of membrane model and the tank track model can be made. The failure of our experiment to detect a retrograde lipid flow validates the conclusion of Sheetz *et al.* (*9*) that such a flow does not drive rearward movements of membrane glycoproteins and so further implicates cytoskeletal involvement in these movements (*16, 17, 24*).

The direct demonstration of lipid flow in moving cells provides an essential missing link in our knowledge of cell locomotion. Although this result applies specifically to the "amoeboid" movements of white blood cells, the basic phenomenon of locomotion is common to most eukaryotic cells and so our findings should also apply to these cells. Thus, it appears that the RLF hypothesis is no longer tenable as a general model for cell locomotion.

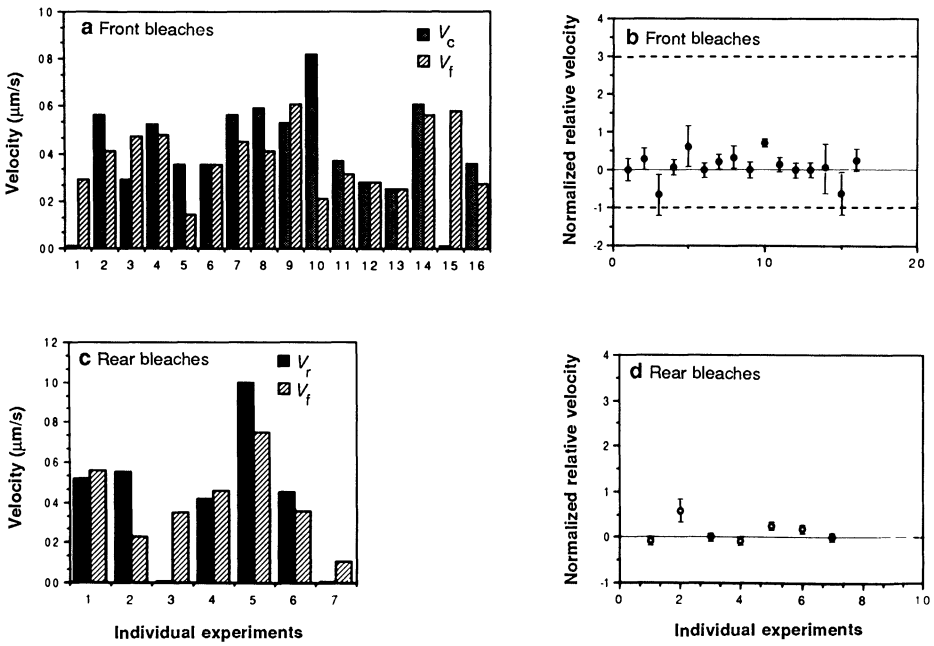

Fig. 4. Velocities of the bleached line and the closest moving edge. (**a**) A histogram of the velocity of the bleached line (V_f, hatched bar) and the velocity of the leading lamella during extension (V_c, stippled bar). Each pair of bars represents one bleached PMN. Note that generally the velocity of the bleached line closely matches the velocity of the leading edge. (**c**) A similar representation of the velocities of a "rear" bleach (V_f, hatched bar) and the rear margin of the cell (V_r, solid bar) during retraction. The velocities of these two regions are similar in most cases. (**b** and **d**) Scatterplots of the normalized relative velocities R for bleached lines relative to the leading lamella and rear of the cell, respectively [$R = (V_c - V_f)/V_c$, front, or $R = (V_r - V_f)/V_r$, rear]. For both front and rear bleaches the normalized relative velocity is about zero. The error bars represent uncertainty in the measurement that arises because the position of the midpoint of the bleached line, the front and rear edge of the cell, are sometimes indistinguishable over 2 to 3 pixels. The error bar represents the maximum and minimum percentage by which R can vary for each photobleaching experiment, depending on the choice of pixel. Uncertainties were obtained by propagating this error through the calculation of R. The dotted lines at $+3$ and -1 represent the expected normalized relative velocities for the RLF and tank track (dorsal surface only) models, respectively (*21, 22*).

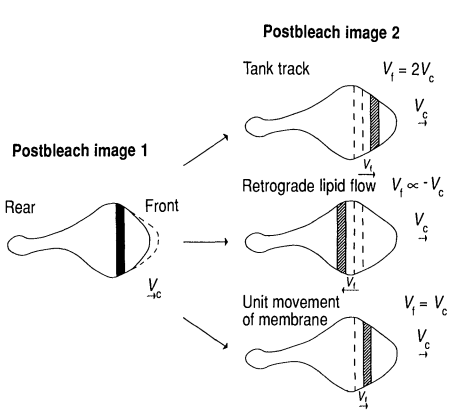

Fig. 5. Predicted second-postbleach images according to three different models of cell locomotion. The solid bar represents the original bleached line. Its original position in the second-postbleach image is represented by the shaded bar and its predicted position is represented by the hatched bar. Each model leads to different predictions about the position of the bleached line in postbleach image 2. The cell velocity (V_c) is the same in each case (arrowed); only the speed and direction of membrane lipid flow (V_f) differs. In the tank track model, the lipid flow velocity on the dorsal surface is assumed to be twice the velocity of the cell (*11*), so that a bleached line on this surface only would advance towards the leading lamella. In contrast, the RLF model assumes that the membrane lipid on dorsal and ventral surfaces flows rearward at about twice the velocity that the cell advances (*1, 12*). A bleached line would then move rearward, away from the leading lamella. In the unit movement of membrane model, lipid on dorsal and ventral surfaces is assumed to flow forward at the same rate as cell advancement without any relative movement between the bleached line and the edge of the leading lamella.

REFERENCES AND NOTES

1. M. Abercrombie, J. E. M. Heaysman, S. M. Pegrum, *Exp. Cell. Res.* **62**, 389 (1970); A. Harris and G. Dunn, *ibid.* **73**, 519 (1972).
2. R. B. Taylor, W. P. H. Duffus, M. C. Raff, S. De Petris, *Nature New Biol.* **233**, 225 (1971).
3. Y. L. Wang, *J. Cell Biol.* **99**, 1478 (1984).
4. R. L. De Biasio, L. L. Wang, G. W. Fisher, D. L. Taylor, *ibid.* **107**, 2631 (1988).
5. P. Forscher and S. J. Smith, *ibid.* **104**, 1505 (1988).
6. A. Ishihara, B. Holifield, K. Jacobson, *ibid.* **106**, 329 (1988).
7. B. Holifield, A. Ishihara, K. Jacobson, unpublished results.
8. M. DeBrabander *et al.*, in *New Methods in Optical Microscopy for Biology*, B. Herman and K. Jacobson, Eds. (Liss, New York, in press).
9. M. P. Sheetz, S. Turney, H. Qian, E. Elson, *Nature* **340**, 284 (1989).
10. D. F. Kucik, E. Elson, M. P. Sheetz, *ibid.*, p. 315.
11. J. M. Lackie, in *Cell Movement and Cell Behaviour*, J. M. Lackie, Ed. (Allen & Unwin, London, 1986), p. 165.
12. M. S. Bretscher, *Science* **224**, 681 (1984).
13. D. Bray and J. G. White, *ibid.* **239**, 883 (1988).
14. S. J. Smith, *ibid.* **242**, 708 (1988).
15. T. Mitchison and M. Kirschner, *Neuron* **1**, 761 (1988).
16. J. P. Heath, *J. Cell Sci.* **60**, 331 (1983); *Nature* **302**, 532 (1983).
17. G. W. Fisher, P. A. Conrad, R. L. DeBiaso, D. L. Taylor, *Cell Motil. Cytoskeleton* **11**, 235 (1988).
18. Similar results were obtained in preliminary bleaching experiments with a different lipid analog, 1-acyl-2-[*N*-(nitrobenzo-2-oxa-1,3-diazole-aminocaproyl) phosphatidylcholine] (NBD-PC). In addition, confocal microscopy (Phoibos 1000, Sarastro) of NBD-

PC–stained cells showed that this analog remains on the cell surface during the experiment.
19. With our present setup, we find the divergence of the laser beam to be no greater than 0.4 μm for 1 μm either side of the plane of focus. Assuming the leading lamella is 1 μm thick, a bleached line of width 4 μm focused on the dorsal surface may be expected to broaden by 10% (4.4 μm) on the ventral surface.
20. Computer simulation has revealed that a broadening of the bleached line recovery profile (2.7 s after photobleaching) of no greater than 6% would be expected for cells moving at speeds between 30 to 60 μm/min, where one surface was assumed to be stationary with respect to the other. In the experimental situation the majority of cells are moving slower than 30 μm/min and so line broadening would be less than 6%. Such a small amount of broadening would be very difficult to detect above experimental variation or noise. A greater broadening of simulated bleached lines occurs at a later time after photobleaching but this corresponds to the virtual completion of diffusional recovery.
21. Particles and concanavalin A attached to the dorsal surface of motile fibroblasts have been observed to move rearward at about twice the velocity of forward protrusion (*1, 12*). Thus if the velocity of membrane lipid flow (V_f) = −2 and the velocity of cell advancement (V_c) = +1, then the normalized relative velocity $R = (V_c - V_f)/V_c = +3$.
22. As in (*21*), if $V_f = +2$ and $V_c = +1$, then the normalized relative velocity, $R = -1$.
23. D. F. Kucik, E. Elson, M. P. Sheetz, *J. Cell Biol.* **109**, 72a (1989).
24. P. Forscher and S. J. Smith, in *Optical Microscopy for Biology*, B. Herman and K. Jacobson, Eds. (Liss, New York, in press).
25. Human PMNs were isolated from a drop of blood by allowing cells to sediment onto a glass cover slip for 20 min at 37°C. The blood clot and any nonadhering cells were washed off the cover slip with warm phosphate-buffered saline (PBS), leaving a population of adherent leukocytes, of which 95% or more are PMNs. A solution of diI in PBS (0.5 μg/ml) was made from a stock solution of diI in absolute ethanol (1 mg/ml) and sonicated for 1 min. Cells were stained with diI for 7 min in the dark at room temperature and then washed three times with warm PBS to remove excess diI. The cells were mounted face up on a microscope slide in culture medium [Dulbecco's minimum essential medium (F/2)] containing 10% fetal bovine serum. A larger cover slip was placed over the cells, supported by a strip of parafilm on either side and sealed with wax to form a small chamber. The slide was placed face down on the microscope stage, which was maintained at 37°C by an air curtain incubator.
26. J. DiGuiseppi, R. Inman, A. Ishihara, K. Jacobson, B. Herman, *Biotechniques* **3**, 394 (1985).
27. H.-G. Kapitza, G. McGregor, K. Jacobson, *Proc. Natl. Acad. Sci. U.S.A.* **82**, 4127 (1985).
28. Cells were stained with diI, washed with warm PBS (as described in Fig. 1), then placed in culture medium with serum and incubated in the dark at 37°C for increasing times after staining (from 10 to 90 min). Cells were then mounted on slides in fresh cooled medium (4°C) and kept on ice until ready for use. Cells were cooled to halt locomotion and to keep further internalization of diI to a minimum. Cells were viewed with a Zeiss laser scanning confocal microscope, at 488 nm with a ×63 oil immersion objective. Digitized images were collected using a Matrox IP512 imaging system and recorded on 35-mm film with a Polaroid freeze-frame color recording system. Each image is an average of four to eight frames.
29. K. Jacobson, Y. Hou, Z. Derzko, J. Wojcieszyn, D. Organisciak, *Biochemistry* **20**, 5268 (1981).
30. Supported by NIH GM35325 and the Swedish Medical Research Council (project no. 6251 and visiting scientist fellowship awarded to K.J., no. K85-16V-7347-01); the Erna and Victor Hasselblad Foundation; the Knut and Alice Wallenberg Foundation; Swedish National Board for Technical Development (no. 87-248P), Magn. Berqvall Fond; the Swedish Society for Medical Research, and Carl Trygger Scientific Foundation. We thank A. Ishihara and T. Sundqvist for help in designing various computer programs used in this project and K. B. Pryzwansky for advice. K.J. especially thanks members of the Department of Medical Microbiology, University of Linköping, for their hospitality during a brief sabbatical where this project was initiated.

We thank C. R. Bagnell for assistance in the use of the confocal microscope (Department of Pathology, School of Medicine, UNC-CH).

6 October 1989; accepted 12 January 1990

Selectivity Changes in Site-Directed Mutants of the VDAC Ion Channel: Structural Implications

ELIZABETH BLACHLY-DYSON, SONGZHI PENG, MARCO COLOMBINI, MICHAEL FORTE*

The gene encoding the yeast mitochondrial outer membrane channel VDAC was subjected to site-directed mutagenesis to change amino acids at 29 positions to residues differing in charge from the wild-type sequence. The mutant genes were then expressed in yeast, and the physiological consequences of single and multiple amino acid changes were assessed after isolation and insertion of mutant channels into phospholipid bilayers. Selectivity changes were observed at 14 sites distributed throughout the length of the molecule. These sites are likely to define the position of the protein walls lining the aqueous pore and hence, the transmembrane segments. These results have been used to develop a model of the open state of the channel in which each polypeptide contributes 12 β strands and one α helix to form the aqueous transmembrane pathway.

VOLTAGE-GATED ION CHANNELS are a class of transmembrane proteins that form aqueous pores in cell membranes—pores that open and close in response to changes in transmembrane voltage and change the ionic permeability of the membrane. Although such channels have been studied primarily in neurons and muscle cells, they are involved in a wide variety of biological processes in many cell types (*1, 2*). Whereas the more extensively studied voltage-gated channels, Na^+ and K^+ channels for example, are high molecular weight protein complexes that form narrow aqueous pores, the mitochondrial voltage-dependent anion-selective channel (VDAC, also known as mitochondrial porin), forms a large voltage-gated pore (*3, 4*) with a relatively small amount of protein (*5*), thus simplifying molecular studies and their interpretation. In addition, since VDAC is found in the yeast *Saccharomyces cerevisiae* (*6*), as well as in the outer mitochondrial membranes of organisms from all eukaryotic kingdoms (*7*), it can be studied with the sophisticated molecular genetic techniques available in this unicellular eukaryote. We have used these techniques to probe the structure of the VDAC molecule and examine the molecular correlates of its biophysical properties.

The VDAC forms large, voltage-gated channels when incorporated into planar phospholipid membranes. It is believed to form the pathway through which metabolic intermediates [for example, adenosine triphosphate (ATP), adenosine diphosphate (ADP), and succinate] enter and leave the mitochondrion (*4*). Measurements of the pore size of VDAC by the Stokes-Einstein radius of the largest nonelectrolyte able to pass through the channel (*8*) and by electron microscopy of negatively stained channels (*9*) indicate that the pore is about 3 nm in diameter. The yeast protein that forms this channel consists of 283 amino acid residues (molecular weight, 29,883) (*10, 11*). The sequence is rather hydrophilic (45.5% charged and polar residues), which is consistent with it being a low molecular weight protein that forms a large aqueous pore with thin walls. It contains no hydrophobic region long enough to span the bilayer as an α helix. The sequence contains many stretches of alternating hydrophobic and hydrophilic residues, which could form a β sheet with hydrophobic residues protruding on one side and hydrophilic residues on the other. This has led to a model of the VDAC channel as a β barrel consisting of a single layer of such a β sheet (*11*). By searching for the most likely transmembrane β strands, 12 probable membrane-spanning stretches have been identified (*12*). The NH_2-terminal 20 residues of VDAC could form an amphipathic α helix typical of mitochondrial tar-

E. Blachly-Dyson and M. Forte, Vollum Institute for Advanced Biomedical Research, Oregon Health Sciences University, Portland, OR 97201.
S. Peng and M. Colombini, Laboratories of Cell Biology, Department of Zoology, University of Maryland, College Park, MD 20742.

*To whom correspondence should be addressed.